JACS
JOURNAL OF THE AMERICAN CHEMICAL SOCIETY
Article
pubs.acs.org/JACS

Structures of Oligomers of a Peptide from β-Amyloid

Johnny D. Pham,[†] Nicholas Chim,[‡] Celia W. Goulding,[‡,§] and James S. Nowick*,[†]

[†]Department of Chemistry, University of California, Irvine, Irvine, California 92697-2025, United States
[‡]Department of Molecular Biology and Biochemistry, University of California, Irvine, Irvine, California 92697-3900, United States
[§]Department of Pharmaceutical Sciences, University of California, Irvine, Irvine, California 92697-3900, United States

Supporting Information

ABSTRACT: Amyloid oligomers play a central role in Alzheimer's and other amyloid diseases, and yet the structures of these heterogeneous and unstable species are not well understood. To better understand the structures of oligomers formed by amyloid-β peptide (Aβ), we have incorporated a key amyloidogenic region of Aβ into a macrocyclic peptide that stabilizes oligomers and facilitates structural elucidation by X-ray crystallography. This paper reports the crystallographic structures of oligomers and oligomer assemblies formed by a macrocycle containing the $A\beta_{15-23}$ nonapeptide. The macrocycle forms hydrogen-bonded β-sheets that assemble into cruciform tetramers consisting of eight β-strands in a two-layered assembly. Three of the cruciform tetramers assemble into a triangular dodecamer. These oligomers further assemble in the lattice to form hexagonal pores. Molecular modeling studies suggest that the natural Aβ peptide can form similar oligomers and oligomer assemblies. The crystallographic and molecular modeling studies suggest the potential for interaction of the oligomers with cell membranes and provide insights into the role of oligomers in amyloid diseases.

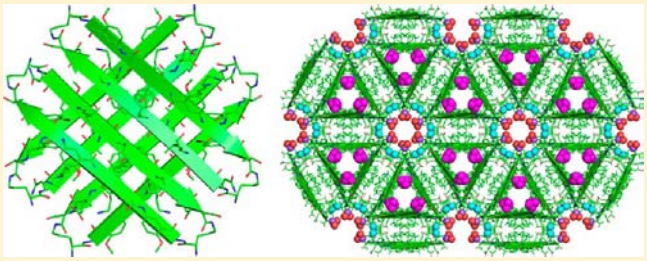

INTRODUCTION

The structures of the toxic amyloid oligomers associated with neurodegenerative diseases remain largely elusive. The plaques formed by amyloid-β peptide (Aβ) are a visible hallmark of Alzheimer's disease, and their component fibrils have been found to consist of long networks of layered β-sheets comprising thousands of molecules of the 40- and 42-amino acid polypeptide.[1−3] Smaller oligomers, consisting of as few as two molecules or as many as tens of molecules, are now widely thought to be the Aβ species that cause neurodegeneration.[4−12] The mechanism or mechanisms by which these oligomers cause neurodegeneration are still not certain, with possibilities including binding to cell-surface receptors, generation of pores of channels in cell membranes, or otherwise perturbing membrane structure.[11]

The structures of the oligomers formed by Aβ and other amyloidogenic peptides and proteins are difficult to study because amyloid oligomers are heterogeneous and unstable. Small oligomers of Aβ, including dimers, trimers, tetramers, hexamers, and dodecamers, have been observed, as well as larger oligomer assemblies with spherical and annular morphologies.[13−19] Most efforts to study the oligomers have relied upon techniques that provide relatively little structural information, such as gel electrophoresis, size-exclusion chromatography, ion mobility mass spectrometry, transmission electron microscopy, atomic force microscopy, and use of oligomer-specific antibodies. Determining the structure of the oligomers of full-length Aβ at atomic resolution simply is not possible. Chemical model systems that are simpler than full-length Aβ can interact in controlled fashions to form well-defined oligomers and oligomer assemblies. These model systems can afford structures at atomic resolution that provide insights into the structures and modes of assembly of amyloid oligomers.

Thus far, there are no chemical model systems that provide deep insights into the structures of Aβ oligomers at atomic resolution. Model systems containing sequences derived from amyloidogenic peptides and proteins have provided glimpses of hydrogen bonding and hydrophobic interactions and geometrical aspects in amyloid oligomer formation.[20−27] Pioneering work by Eisenberg and co-workers revealed the structure of a small toxic oligomer of amyloidogenic peptides derived from the protein αB crystallin to be a barrel-shaped hexamer consisting of six β-strands hydrogen bonded to form a cylindrical β-sheet.[26]

In the current study we set out to observe oligomers and oligomer assemblies formed by the important central region of Aβ by incorporating residues 15−23 into a macrocycle containing a molecular template that controls intermolecular association and blocks the formation of fibrils. To reduce this idea to practice, we combined the nonapeptide QKLVFFAED ($A\beta_{15-23}$) with the unnatural amino acid Hao,[28] two δ-linked ornithine turn units,[29] and three additional amino acids in a 66-membered ring to create macrocyclic peptide **1**. We incorporated a *p*-bromophenylalanine (F^{Br}) residue to facilitate

Received: July 5, 2013
Published: August 8, 2013

   dx.doi.org/10.1021/ja4068854 | J. Am. Chem. Soc. 2013, 135, 12460−12467

phase determination of the X-ray crystallographic structure through single anomalous dispersion (SAD) phasing. We prepared homologues with F^{Br} at several different positions, and ultimately macrocycle **1** afforded crystals suitable for X-ray crystallography.

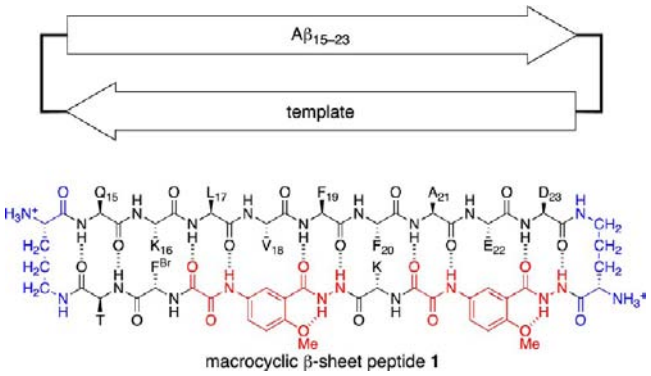

RESULTS

Macrocyclic peptide **1** was synthesized by Fmoc-based solid-phase synthesis of the turn, template, and Aβ_{15-23} units on chlorotrityl resin, followed by cleavage of the protected peptide from the resin, solution-phase cyclization, deprotection, and purification by RP-HPLC (Figures S1 and S2 in Supporting Information). Crystallization conditions were identified by sparse-matrix crystal screening followed by optimization. Crystals were grown in 0.5 M sodium citrate buffer at pH 7.2 with 35% *tert*-butanol and 1% PEG 3350. An X-ray diffraction data set was collected at the bromine absorption edge for SAD phasing. The structure was solved and refined in space group *P*622 at 1.77 Å resolution to give a model with R_{work} = 22.4% and R_{free} = 27.1% (Figure 1 and Table 1). Each asymmetric unit was found to contain a single molecule of macrocyclic peptide **1**. One molecule of *tert*-butanol (*t*-BuOH), two molecules of water, and one sodium ion at 50% occupancy on a 2-fold axis were included in each asymmetric unit.

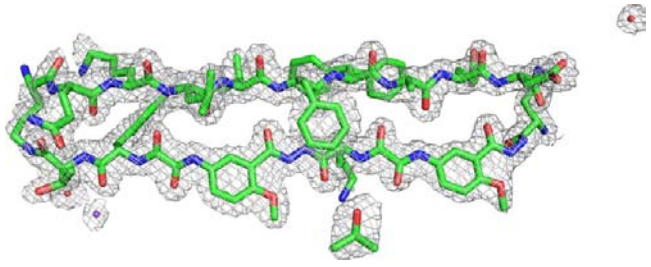

Figure 1. X-ray crystallographic structure and electron density map of the asymmetric unit of macrocyclic *β*-sheet peptide **1**. A $2F_o - F_c$ difference map contoured at 1σ is shown in gray mesh. Macrocyclic *β*-sheet peptide **1** and *tert*-butanol are shown as sticks. Two molecules of water are shown as red spheres. One sodium ion at 50% occupancy on a 2-fold axis is shown as a purple sphere.

The X-ray crystallographic structure of macrocyclic peptide **1** shows a folded monomer that forms hydrogen-bonded dimers, which further assemble to form the crystal lattice. The Aβ_{15-23} nonapeptide adopts a *β*-strand conformation and forms 10 intramolecular hydrogen bonds with the template to make a cyclic *β*-sheet (Figure 2A). The side chains of the nonapeptide project above and below the plane of the *β*-sheet, with the side chains of Q_{15}, L_{17}, F_{19}, A_{21}, and D_{23} projecting on the upper face and the side chains of K_{16}, V_{18}, F_{20}, and E_{22} projecting on the lower face. The side chain of F_{20} exhibits partial occupancy of two rotamers with χ_1 of 176° and 310°.

Table 1. X-ray Crystallographic Data Collection and Refinement Statistics for Macrocyclic *β*-Sheet Peptide 1

Crystal Parameters	
space group	*P*622
a, *b*, *c* (Å)	45.1, 45.1, 29.2
α, β, γ (deg)	90, 90, 120
molecules per asymmetric unit	1
Data Collection	
synchrotron beamline	ALS beamline 8.2.1
wavelength (Å)	0.92
resolution (Å)	50−1.77 (1.83−1.77)
total reflections	38242
unique reflections	1909
completeness (%)[a]	98.8 (96.7)
multiplicity[a]	20.0 (17.8)
R_{merge} (%)[a,b]	12.3 (45.6)
$I/\sigma(I)$[a]	16.8 (8.87)
Refinement	
resolution (Å)	1.77
R_{work} (%)[c]	22.4
R_{free} (%)[d]	27.1
rms bond length (Å)	0.029
rms bond angle (deg)	2.81
ligand	*tert*-butanol (1), sodium (1)
water	2
Ramachandran favored (%)	100
Ramachandran outliers (%)	0
Wilson *B*-factor (Å^2)	32.8
average *B*-factor (Å^2)	42.1

[a]Statistics for the highest resolution shell are shown in parentheses. [b]$R_{merge} = \sum|I - \langle I\rangle|/\sum I$. [c]$R_{work} = \sum||F_{obs}| - |F_{calc}||/\sum|F_{obs}|$. [d]$R_{free}$ was computed identically as R_{work} except where all reflections belong to a test set of 8% randomly selected data.

Macrocyclic *β*-sheet peptide **1** forms a hydrogen-bonded dimer in which the two Aβ_{15-23} nonapeptide strands align and form eight hydrogen bonds to make a four-stranded antiparallel *β*-sheet (Figure 2B).[30−34] The hydrophobic side chains of L_{17}, F_{19}, and A_{21} make a hydrophobic patch that is flanked by the polar side chains of Q_{15} and D_{23} on the upper face of the *β*-sheet (Figure 2C); the hydrophobic side chains of V_{18} and F_{20} make a hydrophobic patch that is flanked by the polar side chains of K_{16} and E_{22} on the lower face of the *β*-sheet (Figure 2D). We term the upper and lower faces the *LFA face* and the *VF face* for the subsequent discussion of the assembly of the dimers.

The hydrogen-bonded dimers pack in a hexagonal fashion to form the crystal lattice (Figure 3A). The lattice has triangular and hexagonal cavities, which are readily apparent in a space-filling model (Figure 3B). The LFA faces line the triangular cavities, while the VF faces pack to create a hydrophobic network that separates the triangular cavities. The polar residues (Q_{15}, K_{16}, E_{22}, and D_{23}) and *δ*-linked ornithine turn units meet at the hexagonal cavities. The triangular cavities are about 1 nm across, while the hexagonal cavities are about 1.5 nm in diameter. The *t*-BuOH resides in the hydrophobic triangular cavities, while the sodium ion and water reside in the hydrophilic hexagonal cavities (Figure 3C).

dx.doi.org/10.1021/ja4068854 | J. Am. Chem. Soc. 2013, 135, 12460−12467

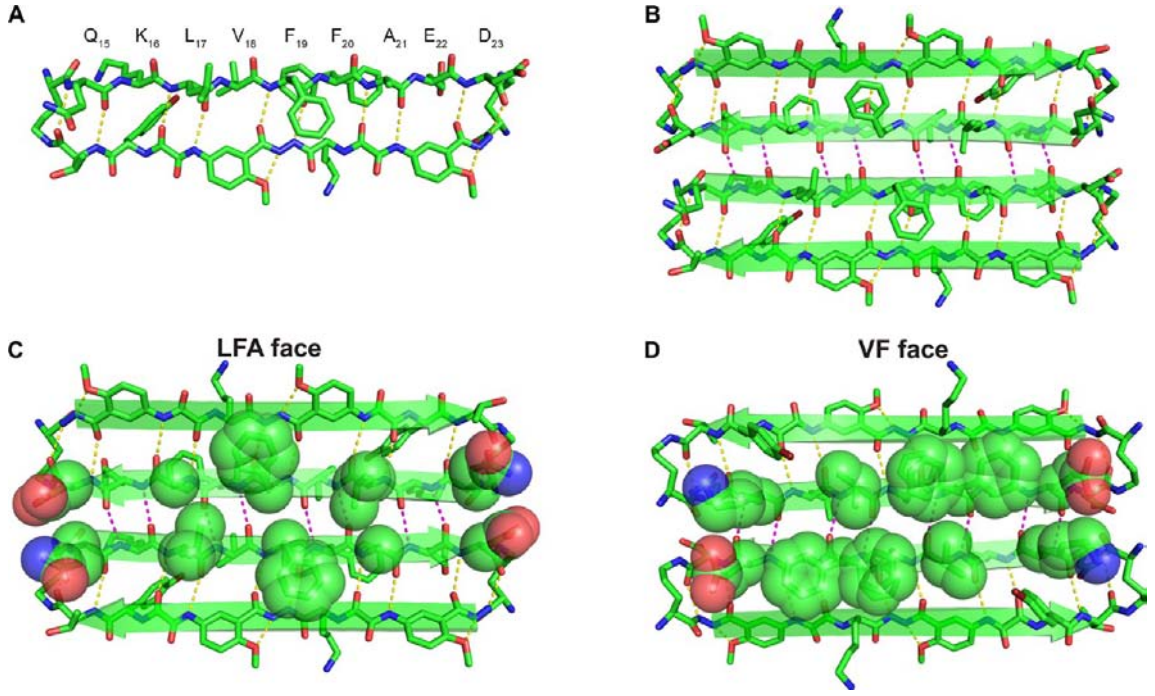

Figure 2. X-ray crystallographic structure of macrocyclic β-sheet peptide **1**. (A) Monomeric subunit. (B) Hydrogen-bonded dimer. (C) Hydrogen-bonded dimer illustrating relationship of Q_{15}, L_{17}, F_{19}, A_{21}, and D_{23} (LFA face view). (D) Hydrogen-bonded dimer illustrating relationship of K_{16}, V_{18}, F_{20}, and E_{22} (VF face view). The side chain of F_{20} exhibits partial occupancy of two rotamers; both rotamers are shown.

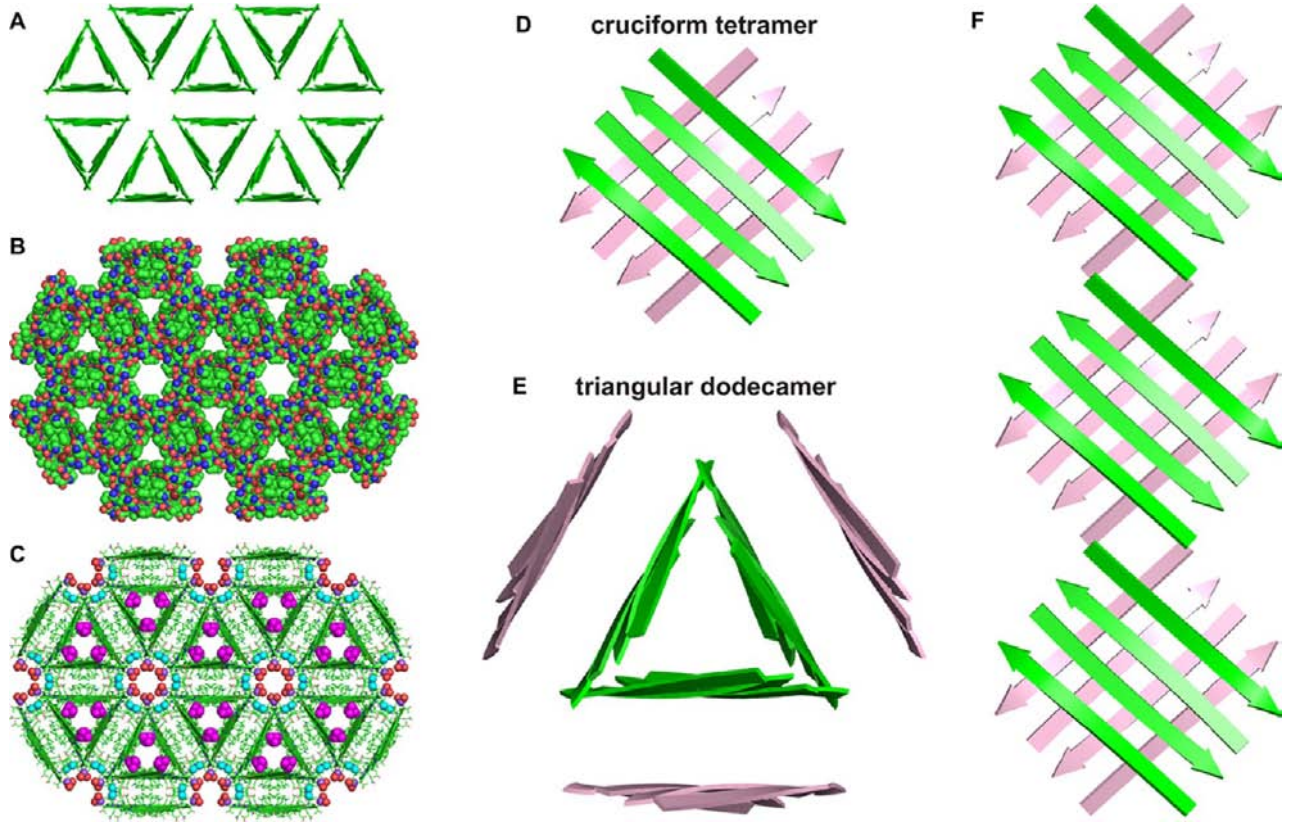

Figure 3. Crystal packing of macrocyclic β-sheet peptide **1**. (A) Crystal lattice (cartoon, top view). (B) Crystal lattice (space filling model, top view). (C) Crystal lattice showing solvent and ions (top view): *t*-BuOH (magenta, in the triangular cavities), Na^+ (purple, in the hexagonal cavities), H_2O ligands for Na^+ (red, in the hexagonal cavities), additional H_2O (cyan, in the hexagonal cavities). (D) Cruciform tetramer within the crystal lattice (side view). (E) Triangular dodecamer within the crystal lattice comprising three tetrameric subunits (top view). (F) Linear assembly of tetramers within the crystal lattice (side view). Three tetrameric subunits of the infinite linear assembly are shown.

dx.doi.org/10.1021/ja4068854 | *J. Am. Chem. Soc.* 2013, 135, 12460−12467

The lattice may be thought of as comprising two types of oligomers: *cruciform tetramers* and *triangular dodecamers*. The hydrogen-bonded dimers pack through the VF faces to create tetramers (Figure 3D and Figure S3A,B). In the tetramers the β-sheets of the dimers are nearly orthogonal, oriented at an 83° angle. These cruciform tetramers are about 3 nm wide and 2 nm thick. The V_{18} and F_{20} side chains pack through hydrophobic and aromatic interactions, and aromatic stacking interactions occur between the side chains of the bromophenylalanine residues. These interactions help stabilize the tetramer.

Three cruciform tetramers pack in a triangular arrangement to form a triangular dodecamer (Figure 3E and Figure S3C). The dodecamer is about 4−5 nm across and 3 nm thick. The L_{17}, F_{19}, and A_{21} side chains line the interior of the triangular dodecamer, creating a hydrophobic cavity. The three interior walls of the dodecamer (shown in green in Figure 3E) and three exterior walls of the dodecamer (shown in pink in Figure 3E) each consist of the hydrogen-bonded dimers of macrocyclic β-sheet peptide **1**. The F^{Br} residues abut at the juncture between the interior walls, forming a weak pair of hydrogen bonds (Figure 4).

The cruciform tetramers fit together to form infinite linear assemblies that run through the lattice (Figure 3F). The β-sheet interfaces between the tetramer units are shifted out of alignment by six residues toward the N-termini. The Hao units of the template strands abut at the interface between tetramer units, creating an overlap equivalent in length to three residues but without any hydrogen bonds (Figure S4). The triangular cavities are formed from the convergence of three such infinite linear assemblies and may be thought of as infinite stacks of triangular dodecamers that run through the lattice.

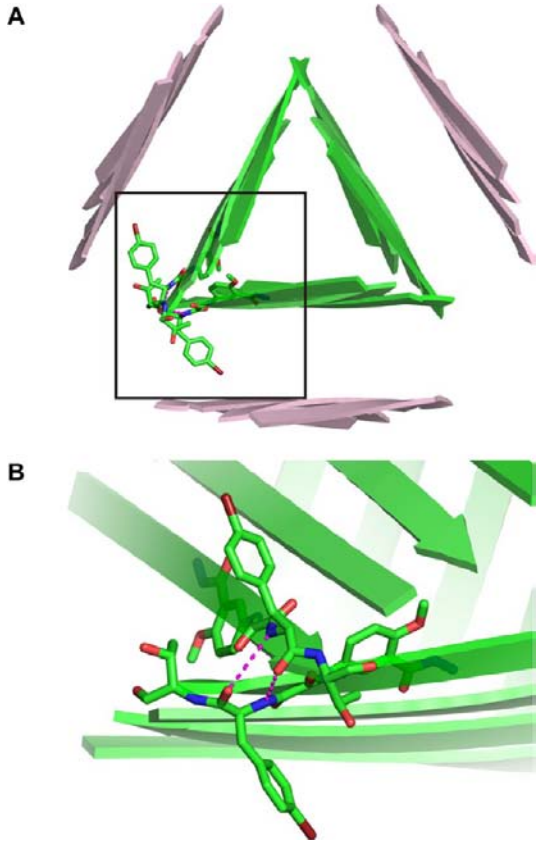

Figure 4. Contacts between the cruciform tetramer units of the triangular dodecamer in the X-ray crystallographic structure of macrocyclic β-sheet peptide **1**: (A) triangular dodecamer formed by three tetramer subunits; (B) detail of the contact between two cruciform tetramer units of the triangular dodecamer showing hydrogen bonding between the F^{Br} residues.

DISCUSSION

To envision how the X-ray crystallographic structure of macrocyclic β-sheet peptide **1** reflects the structures of amyloid oligomers of natural peptides and proteins, we used the structure to model assemblies of $A\beta_{15-23}$ homologous to the cruciform tetramer, the triangular dodecamer, and the linear assembly of tetramers. We modeled each of these assemblies by replacing the QKLVFFAED nonapeptide strand and the template strand of macrocyclic β-sheet peptide **1** with linear peptide **2** (Ac-QKLVFFAED-NHMe, Ac-$A\beta_{15-23}$-NHMe) and generating a minimum energy structure using molecular mechanics with the Merck molecular force field (MMFF) and GB/SA water solvation (Figure S5). Figure 5 illustrates the resulting structures of the 8-stranded cruciform oligomer, 24-stranded triangular oligomer, and linear assembly of cruciform oligomers modeled with linear peptide **2**.

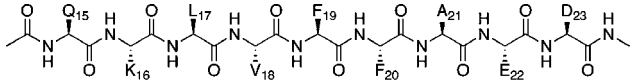

linear peptide **2**

The cruciform oligomer modeled from linear peptide **2** consists of two four-stranded antiparallel β-sheets packed through hydrophobic interactions (Figure 5A). In each four-stranded antiparallel β-sheet, the hydrophobic side chains of L_{17}, F_{19}, and A_{21} make a hydrophobic patch that is flanked by the polar side chains of Q_{15} and D_{23} on the LFA face (Figure 5B), and the hydrophobic side chains of V_{18} and F_{20} make a hydrophobic patch that is flanked by the polar side chains of K_{16} and E_{22} on the VF face (Figure 5C). The two four-stranded antiparallel β-sheets pack through the VF faces and are nearly orthogonal. The methylene groups of the K_{16} and E_{22} side chains may further pack with the V_{18} and F_{20} side chains to stabilize the hydrophobic core of the cruciform oligomer.

The width of each four-stranded β-sheet is roughly comparable to the length of the seven-amino acid β-strand region from K_{16} to E_{22}, each is about 2 nm. The formation of a cruciform structure between these two β-sheets may reflect a general mode of β-sheet interaction in amyloid oligomers, in which β-sheets of about four peptide strands in width and seven amino acids in length assemble in a crisscross fashion through hydrophobic interactions.[24,25] Hydrophobic interactions through either the VF or the LFA face should be possible (Figure S6). Both antiparallel and parallel β-sheets should be able to interact in this fashion (Figure S6). The β-strands comprising the β-sheets may be of the same or different sequences. For example, $A\beta_{16-22}$ (KLVFFAE) should be able to interact both with itself and with hydrophobic sequences from the C-terminal region of $A\beta$, such as $A\beta_{30-36}$ (AIIGLMV).[20,21] Thus, an eight-stranded cruciform oligomer could form from as few as four molecules of $A\beta_{1-40}$ or $A\beta_{1-42}$, with loops connecting the $A\beta_{15-23}$ and C-terminal β-strands (Figure 6).

The triangular oligomer modeled from linear peptide **2** consists of three cruciform oligomers in a triangular arrangement (Figure 5D). The hydrophobic L_{17}, F_{19}, and A_{21} side chains line the triangular cavity, and the hydrophobic V_{18} and

dx.doi.org/10.1021/ja4068854 | J. Am. Chem. Soc. 2013, 135, 12460−12467

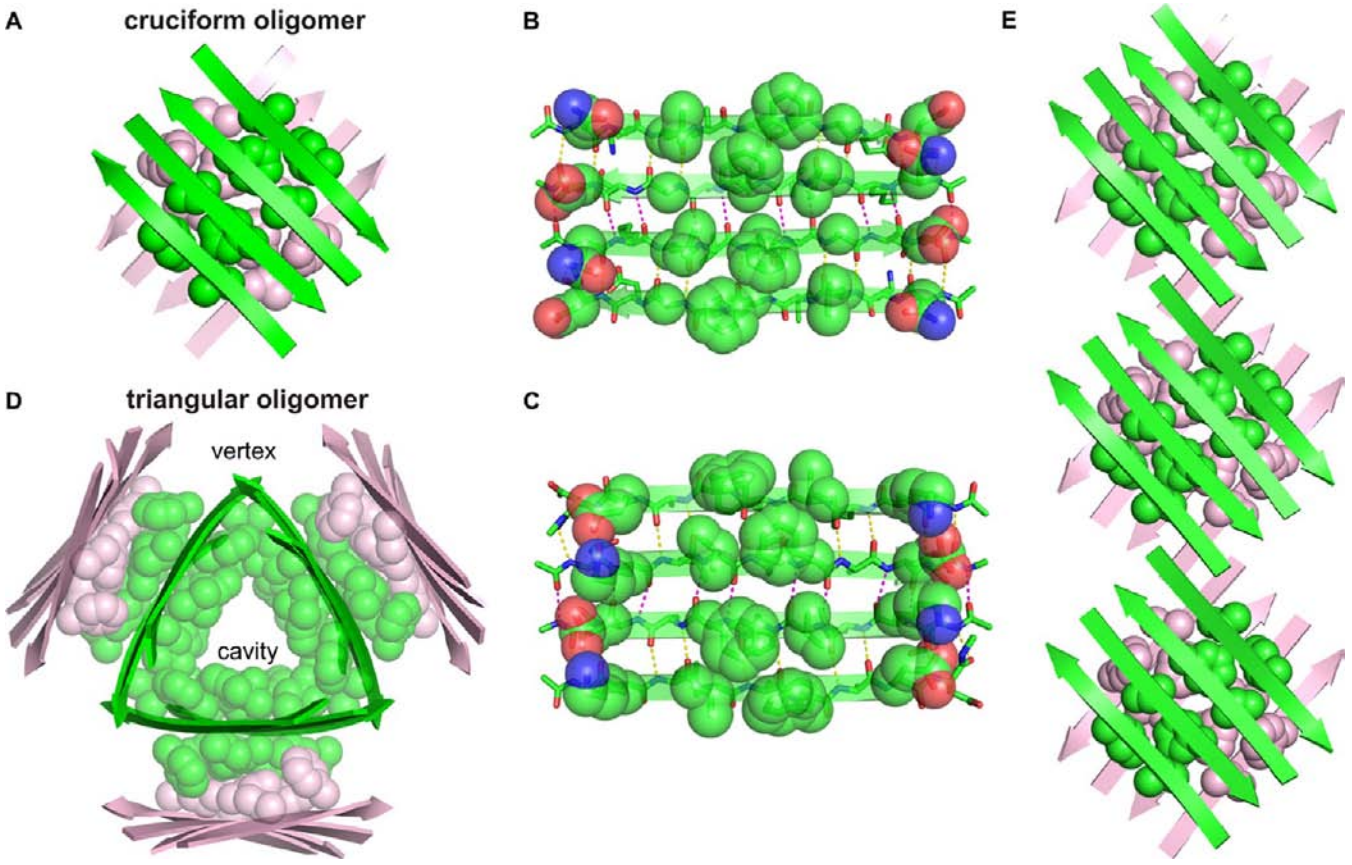

Figure 5. Crystallographically based molecular models of oligomers of Aβ_{15-23}. (A) Eight-stranded cruciform oligomer of linear peptide **2** (Ac-QKLVFFAED-NHMe, Ac-Aβ_{15-23}-NHMe). Model is based upon tetramer of macrocyclic β-sheet peptide **1** (Figure 3D). Side chains of V_{18} and F_{20} in the hydrophobic core are shown. (B) Antiparallel β-sheet comprising four strands of linear peptide **2** (LFA face view). Model is one layer of the eight-stranded cruciform oligomer. (C) Antiparallel β-sheet comprising four strands of linear peptide **2** (VF face view). Model is one layer of the eight-stranded cruciform oligomer. (D) Twenty-four-stranded triangular oligomer of linear peptide **2**. Model is based upon dodecamer of macrocyclic β-sheet peptide **1** (Figure 3E). Side chains of L_{17}, F_{19}, and A_{21} lining the triangular cavity and V_{18} and F_{20} forming the hydrophobic cores between the interior and exterior walls are shown. Side chains of Q_{15}, K_{16}, E_{22}, and D_{23} (not shown) converge at the vertices. (E) Linear assembly of cruciform oligomers of linear peptide **2**. Model is based upon assembly of tetramers of macrocyclic β-sheet peptide **1** (Figure 3F). Side chains of V_{18} and F_{20} in the hydrophobic cores are shown.

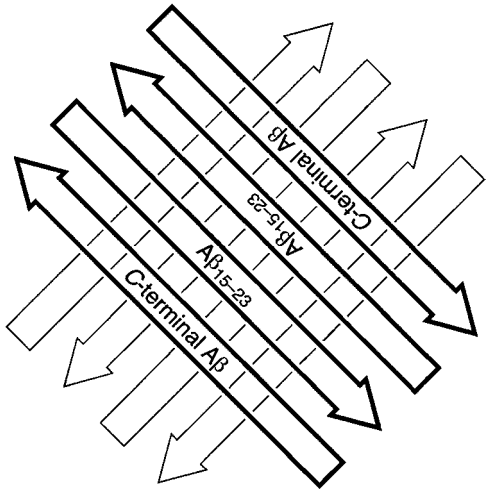

Figure 6. Cartoon of an eight-stranded cruciform oligomer comprising the Aβ_{15-23} and C-terminal β-strands.

F_{20} side chains pack to form the hydrophobic cores between the interior and exterior walls. The E_{22} residues abut at the juncture between the interior walls forming a pair of hydrogen bonds. The polar side chains of Q_{15}, K_{16}, E_{22}, and D_{23} converge at the vertices of the triangles.

In a triangular oligomer formed from Aβ_{1-40} or Aβ_{1-42} the polypeptide chains would extend beyond the vertices (Figure 5D) and create additional stabilizing hydrophobic and polar contacts. The side chains of H_{13} and H_{14} would converge at the vertices, along with those of E_{22} and D_{23}. These side chains would create rich ligating environments for metal ions, which could further stabilize the oligomer, much akin to the sodium ions in the lattice (Figure 3C). Lipids could further stabilize the oligomer by binding inside the triangular cavity, in a fashion similar to the *t*-BuOH in the lattice (Figure 3C). A triangular oligomer formed from Aβ_{1-40} or Aβ_{1-42} need not consist only of the N-terminal hydrophobic region of Aβ and could also incorporate hydrophobic sequences from the C-terminal region. Thus, a triangular oligomer could form from as few as 12 molecules of Aβ_{1-40} or Aβ_{1-42}, with loops connecting the β-strands.

The linear assembly of oligomers modeled from linear peptide **2** consists of three cruciform oligomers in a linear arrangement (Figure 5E). The nonapeptide strands of the cruciform oligomers are shifted out of alignment by six residues at the juncture between the tetramer units. Because the assemblies lack the Hao units, the N-termini of the β-strands at

dx.doi.org/10.1021/ja4068854 | J. Am. Chem. Soc. 2013, 135, 12460−12467

the juncture are able to hydrogen-bond, and each β-strand creates a three-residue hydrogen-bonded β-sheet between the cruciform oligomer units. Assemblies of cruciform oligomers can also occur through overlap of the C-termini of the β-strands (e.g., Figure S7).

The crystal lattice of macrocyclic β-sheet peptide **1** (Figure 3A−C) suggests the potential for incorporation of cruciform and triangular oligomers of Aβ into lipid bilayer membranes. The triangular cavities in the lattice are surrounded by the hydrophobic L_{17}, F_{19}, and A_{21} side chains. The lipophilic *t*-BuOH in these cavities suggests the potential for the oligomers to assemble in lipid bilayer membranes and be stabilized by interactions of the hydrophobic LFA faces with lipids. The hexagonal cavities in the lattice (Figures 3A−C) suggest the potential for the creation of hydrophilic pores in lipid bilayer membranes that could disrupt membrane integrity toward water or ions. The hexagonal cavities in the lattice are surrounded by the polar Q_{15}, K_{16}, E_{22}, and D_{23} side chains. The presence of sodium ions and water in these cavities suggests that six cruciform oligomers or three triangular oligomers could form a hexagonal pore in a membrane that could serve as a conduit for water or metal cations (Figure 7). If oligomers from Aβ_{1-40} or Aβ_{1-42} were to form such pores, the side chains of H_{13} and H_{14} would line the pores, along with those of E_{22} and D_{23}, further facilitating the binding and transport of metal cations. The hexagonal arrangement of oligomers in the crystal lattice appear to be consistent in size and morphology with the hexagonal and annular porelike structures observed for Aβ and other amyloidgenic peptides and proteins.[35−38] The X-ray crystallographic structure of macrocyclic β-sheet **1** may thus provide a glimpse into the molecular basis of Aβ oligomer toxicity.[39−42]

The cruciform and triangular oligomers observed for macrocyclic β-sheet peptide **1** and modeled for linear peptide **2** reflect common themes observed in amyloidogenic peptides. Aβ_{1-40}, Aβ_{1-42}, islet amyloid polypeptide, and small peptides derived from human prions, tau, and insulin form fibrils composed of layered β-sheets.[1−3,43−45] In the fibrils, the β-sheets form long networks of β-strands and the component β-strands are nearly orthogonal to the fibril axis. The cruciform oligomer described here is similar to the fibrils in that it consists of a layered pair of β-sheets with a central hydrophobic core. It differs in that the β-sheets are nearly orthogonal and are composed of only four β-strands apiece. Under suitable conditions, Aβ_{1-40} can form 3-fold symmetrical assemblies consisting of layered pairs of β-sheets in a triangular arrangement around the fibril axis.[3] The triangular oligomer described here is similar to the triangular fibril assemblies in that the 3-fold symmetrical structure consists of layered pairs of β-sheets. It differs in that the β-sheets are at nearly a 45° angle to the 3-fold axis.

The triangular core of the triangular oligomer of macrocyclic β-sheet peptide **1** is a homologated cylindrin, similar to the previously reported barrel-shaped hexamer structure of amyloid oligomers derived from αB crystallin but expanded from 6 β-strands to 12 (Figure S8).[26] The core of the triangular oligomer consists of three four-stranded β-sheet subunits that are hydrogen-bonded to make a cylindrical 12-stranded β-sheet.[27] The β-strands of three β-sheet subunits are fully aligned but are then shifted out of alignment by six residues, toward the C-terminus, at the juncture between the three subunits. In the previously reported cylindrin structures, the junctures between the three aligned two-stranded β-sheet subunits shift out of alignment by two residues, toward the N-terminus, giving a net shift of one residue per β-strand and a right-handed propeller structure. In the triangular core of the triangular oligomer of macrocyclic β-sheet peptide **1**, there is a net shift of one and a half residues per β-strand and a right-handed propeller

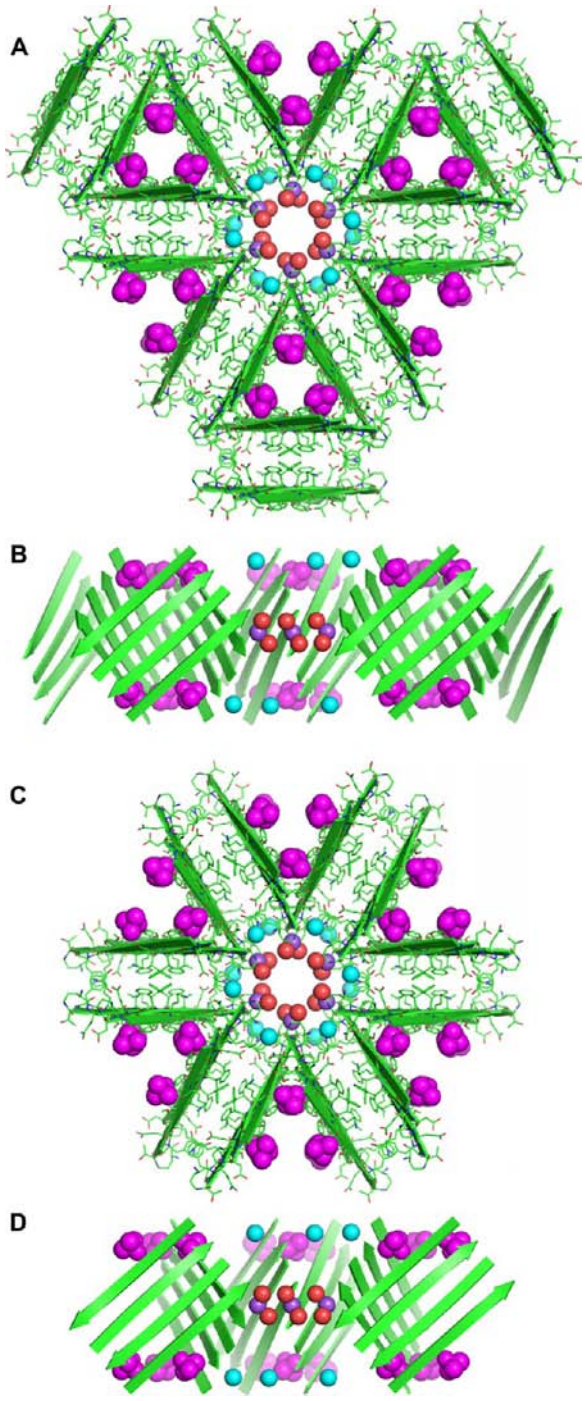

Figure 7. Hexagonal pores within the crystal lattice of macrocyclic β-sheet peptide **1**. (A) Hexagonal pore formed by three triangular dodecamers (top view): *t*-BuOH (magenta, in the triangular cavities), Na^+ (purple, in the hexagonal cavities), H_2O ligands for Na^+ (red, in the hexagonal cavities), additional H_2O (cyan, in the hexagonal cavities). (B) Hexagonal pore formed by three triangular dodecamers (cutaway side view). (C) Hexagonal pore formed by six cruciform tetramers (top view). (D) Hexagonal pore formed by six cruciform tetramers (cutaway side view).

dx.doi.org/10.1021/ja4068854 | J. Am. Chem. Soc. 2013, 135, 12460−12467

structure. As a result of the larger net shift, the β-strands of this cylindrin are at a larger angle with respect to the cylinder axis than those of αB crystallin. This difference may reflect the blocking of hydrogen bonding by the Hao units.

CONCLUSION

The X-ray crystallographic structure of Aβ-derived peptide **1** provides a unique window into the supramolecular assembly of β-amyloid peptides and perhaps amyloidogenic peptides in general. Assembly of peptide strands into small β-sheets that further assemble in a crisscross fashion creates cruciform oligomers. The cruciform oligomers can assemble in a hierarchical fashion to create larger oligomers and oligomer assemblies. Three cruciform oligomers can assemble in a propeller-like fashion to form triangular oligomers. The cruciform oligomers can also assemble in a linear fashion to form linear assemblies. Three triangular oligomers or six cruciform oligomers can assemble to form hexagonal pores lined with hydrophilic ionophoric groups. The hydrophobic surfaces of the cruciform oligomers and oligomer assemblies may provide a means by which these structures can insert into lipid bilayer membranes, facilitate the transport of water or metal cations, and disrupt cellular homeostasis.

ASSOCIATED CONTENT

Supporting Information

Crystallographic data in CIF format and details of the synthesis and crystallization of macrocyclic β-sheet peptide **1**, X-ray diffraction data collection, processing, and structure and refinement, and modeling of oligomers of linear peptide **2**. This material is available free of charge via the Internet at http://pubs.acs.org. The crystal structure of QKLVFFAED nonapeptide segment was deposited into the Protein Data Bank (PDB) with PDB code 4IVH.

AUTHOR INFORMATION

Corresponding Author

jsnowick@uci.edu

Notes

The authors declare no competing financial interest.

ACKNOWLEDGMENTS

We thank Angelina Iniguez for technical assistance in crystallization and crystal harvesting of macrocyclic β-sheet peptide **1**, the staff and facilities of the Advanced Light Source at Lawrence Berkeley National Laboratory for invaluable help in generating and collecting data, Dr. Michael W. Sawaya for assistance in refining the X-ray crystallographic structure of macrocyclic β-sheet peptide **1**, and Professor David Eisenberg for helpful discussions. J.S.N. and J.D.P. thank the National Institutes of Health for grant support (Grant 1R01GM097562). C.W.G. also thanks the National Institutes of Health for grant support (Grant R21AI099687).

REFERENCES

(1) Lührs, T.; Ritter, C.; Adrian, M.; Riek-Loher, D.; Bohrmann, B.; Döbeli, H.; Schubert, D.; Riek, R. *Proc. Natl. Acad. Sci. U.S.A.* **2005**, *102*, 17342−17347.
(2) Petkova, A. T.; Yau, W.-M.; Tycko, R. *Biochemistry* **2006**, *45*, 498−512.
(3) Paravastu, A. K.; Leapman, R. D.; Yau, W.-M.; Tycko, R. *Proc. Natl. Acad. Sci. U.S.A.* **2008**, *105*, 18349−18354.
(4) Kayed, R.; Head, E.; Thompson, J. L.; McIntire, T. M.; Milton, S. C.; Cotman, C. W.; Glabe, C. G. *Science* **2003**, *300*, 486−489.
(5) Haass, C.; Selkoe, D. J. *Nat. Rev. Mol. Cell Biol.* **2007**, *8*, 101−112.
(6) Walsh, D. M.; Selkoe, D. J. *J. Neurochem.* **2007**, *101*, 1172−1184.
(7) Selkoe, D. J. *Behav. Brain Res.* **2008**, *192*, 106−113.
(8) Glabe, C. G. *J. Biol. Chem.* **2008**, *283*, 29639−29643.
(9) Kayed, R.; Canto, I.; Breydo, L.; Rasool, S.; Lukacsovich, T.; Wu, J.; Albay, R., III; Pensalfini, P.; Yeung, S.; Head, E.; Marsh, J. L.; Glabe, C. *Mol. Neurodegener.* **2010**, *5*, 1−10.
(10) Fändrich, M. *J. Mol. Biol.* **2012**, *421*, 427−440.
(11) Benilova, I.; Karran, E.; De Stooper, B. *Nat. Neurosci.* **2012**, *15*, 349−357.
(12) Nussbaum, J. M.; Schilling, S.; Cynis, H.; Silva, A.; Swanson, E.; Wangsanut, T.; Tayler, K.; Wiltgen, B.; Hatami, A.; Rönicke, R.; Reymann, K.; Hutter-Paier, B.; Alexandru, A.; Jagla, W.; Graubner, S.; Glabe, C. G.; Demuth, H.-U.; Bloom, G. S. *Nature* **2012**, *485*, 651−655.
(13) Chen, Y.-R.; Glabe, C. G. *J. Biol. Chem.* **2006**, *281*, 24414−24422.
(14) Lesné, S.; Koh, M. T.; Kotilinek, L.; Kayed, R.; Glabe, C. G.; Yang, A.; Gallagher, M.; Ashe, K. H. *Nature* **2006**, *440*, 352−357.
(15) Shankar, G. M.; Li, S.; Mehta, T. H.; Garcia-Munoz, A.; Shepardson, N. E.; Smith, I.; Brett, F. M.; Farrell, M. A.; Rowan, M. J.; Lemer, C. A.; Regan, C. M.; Walsh, D. M.; Sabatini, B. L.; Selkoe, D. J. *Nat. Med.* **2008**, *14*, 837−842.
(16) Bernstein, S. L.; Dupuis, N. F.; Lazo, N. D.; Wyttenbach, T.; Condron, M. M.; Bitan, G.; Teplow, D. B.; Shea, J.-E.; Ruotolo, B. T.; Robinson, C. V.; Bowers, M. T. *Nat. Chem.* **2009**, *1*, 326−331.
(17) Ono, K.; Condron, M. M.; Teplow, D. B. *Proc. Natl. Acad. Sci. U.S.A.* **2009**, *106*, 14745−14750.
(18) Zhang, R.; Hu, X.; Khant, H.; Ludtke, S. J.; Chiu, W.; Schmid, M. F.; Frieden, C.; Lee, J.-M. *Proc. Natl. Acad. Sci. U.S.A.* **2009**, *106*, 4653−4658.
(19) Miller, Y.; Ma, B.; Tsai, C.-J.; Nussinov, R. *Proc. Natl. Acad. Sci. U.S.A.* **2010**, *107*, 14128−14133.
(20) Hoyer, W.; Grönwall, C.; Jonsson, A.; Ståhl, S.; Härd, T. *Proc. Natl. Acad. Sci. U.S.A.* **2008**, *105*, 5099−5104.
(21) Sandberg, A.; Luheshi, L. M.; Söllvander, S.; de Barros, T. P.; Macao, B.; Knowles, T. P. J.; Biverstål, H.; Lendel, C.; Ekholm-Petterson, F.; Dubnovitsky, A.; Lannfelt, L.; Dobson, C. M.; Härd, T. *Proc. Natl. Acad. Sci. U.S.A.* **2010**, *107*, 15595−15600.
(22) Yu, L.; Edalji, R.; Harlan, J. E.; Holzman, T. F.; Lopez, A. P.; Labkovsky, B.; Hillen, H.; Barghorn, S.; Ebert, U.; Richardson, P. L.; Miesbauer, L.; Solomon, L.; Bartley, D.; Walter, K.; Johnson, R. W.; Hajduk, P. J.; Olejniczak, E. T. *Biochemistry* **2009**, *48*, 1870−1877.
(23) Miller, Y.; Ma, B.; Nussinov, R. *Chem. Rev.* **2010**, *110*, 4820−4838.
(24) Liu, C.; Sawaya, M. R.; Cheng, P.-N.; Zheng, J.; Nowick, J. S.; Eisenberg, D. *J. Am. Chem. Soc.* **2011**, *133*, 6736−6744.
(25) Liu, C.; Zhao, M.; Jiang, L.; Cheng, P.-N.; Park, J.; Sawaya, M. R.; Pensalfini, A.; Gou, D.; Berk, A. J.; Glabe, C. G.; Nowick, J. S.; Eisenberg, D. *Proc. Natl. Acad. Sci. U.S.A.* **2012**, *109*, 20913−20918.
(26) Laganowsky, A.; Liu, C.; Sawaya, M. R.; Whitelegge, J. P.; Park, J.; Zhao, M.; Pensalfini, A.; Soriaga, A. B.; Landau, M.; Keng, P. K.; Cascio, D.; Glabe, C. G.; Eisenberg, D. *Science* **2012**, *335*, 1228−1231.
(27) Apostol, M. I.; Perry, K.; Surewicz, W. K. *J. Am. Chem. Soc.* **2013**, *135*, 10202−10205.
(28) Nowick, J. S.; Chung, D. M.; Maitra, K.; Maitra, S.; Stigers, K. D.; Sun, Y. J. *J. Am. Chem. Soc.* **2000**, *122*, 7654−7661.
(29) Nowick, J. S.; Brower, J. O. *J. Am. Chem. Soc.* **2003**, *125*, 876−877.
(30) Tjernberg, L. O.; Callaway, D. J. E.; Tjernberg, A.; Hahne, S.; Lilliehöök, C.; Terenius, L.; Thyberg, J.; Nordstedt, C. *J. Biol. Chem.* **1999**, *274*, 12619−12625.
(31) Balbach, J. J.; Ishii, Y.; Antzutkin, O. N.; Leapman, R. D.; Rizzo, N. W.; Dyda, F.; Reed, J.; Tycko, R. *Biochemistry* **2000**, *39*, 13748−13759.

(32) Mehta, A. K.; Lu, K.; Childers, W. S.; Liang, Y.; Dublin, S. N.; Dong, J.; Snyder, J. P.; Pingali, S. V.; Thiyagarajan, P.; Lynn, D. G. *J. Am. Chem. Soc.* **2008**, *130*, 9829−9835.
(33) Liang, Y.; Pingali, S. V.; Jogalekar, A. S.; Snyder, J. P.; Thiyagarajan, P.; Lynn, D. G. *Biochemistry* **2008**, *47*, 10018−10026.
(34) Qiang, W.; Yau, W.-M.; Luo, Y.; Mattson, M. P.; Tycko, R. *Proc. Natl. Acad. Sci. U.S.A.* **2012**, *109*, 4443−4448.
(35) Lin, H.; Bhatia, R.; Lal, R. *FASEB J.* **2001**, *15*, 2433−2444.
(36) Lashuel, H. A.; Hartley, D.; Petre, B. M.; Walz, T.; Lansbury, P. T., Jr. *Nature* **2002**, *418*, 291.
(37) Quist, A.; Doudevski, I.; Lin, H.; Azimova, R.; Ng, D.; Frangione, B.; Kagan, B.; Ghiso, J.; Lal, R. *Proc. Natl. Acad. Sci. U.S.A.* **2005**, *102*, 10427−10432.
(38) Kayed, R.; Pensalfini, A.; Margol, L.; Sokolov, Y.; Sarsoza, F.; Head, E.; Hall, J.; Glabe, C. G. *J. Biol. Chem.* **2009**, *284*, 4230−4237.
(39) Lashuel, H. A.; Lansbury, P. T., Jr. *Q. Rev. Biophys.* **2006**, *39*, 167−201.
(40) Butterfield, S. M.; Lashuel, H. A. *Angew. Chem., Int. Ed.* **2010**, *49*, 5628−5654.
(41) Kayed, R.; Sokolov, Y.; Edmonds, B.; McIntire, T. M.; Milton, S. C.; Hall, J. E.; Glabe, C. G. *J. Biol. Chem.* **2004**, *279*, 46363−46366.
(42) Lasagna-Reeves, C. A.; Glabe, C. G.; Kayed, R. *J. Biol. Chem.* **2011**, *286*, 22122−22130.
(43) Luca, S.; Yau, W.-M.; Leapman, R.; Tycko, R. *Biochemistry* **2007**, *46*, 13505−13522.
(44) Nelson, R.; Sawaya, M. R.; Balbirnie, M.; Madsen, A. Ø.; Riekel, C.; Grothe, R.; Eisenberg, D. *Nature* **2005**, *435*, 773−778.
(45) Sawaya, M. R.; Sambashivan, S.; Nelson, R.; Ivanova, M. I.; Sievers, S. A.; Apostol, M. I.; Thompson, M. J.; Balbirnie, M.; Wiltzius, J. J. W.; McFarlane, H. T.; Madsen, A. Ø.; Riekel, C.; Eisenberg, D. *Nature* **2007**, *447*, 453−457.